Archives of Mechanics • Archiwum Mechaniki Stosowanej • 30, 4–5, pp. 337–351, Warszawa 1978

Base pressure oscillations in a rectangular duct with an abrupt enlargement

J. S. ANDERSON (LONDON), G. GRABITZ, G. E. A. MEIER (GÖTTINGEN), W. M. JUNGOWSKI and K. J. WITCZAK (WARSZAWA)

THIS PAPER deals with a study of unsteady, compressible flow in a rectangular duct which follows an abrupt enlargement of section. Sonic flow from a short, two-dimensional convergent nozzle expands into the rectangular duct to provide a mixed, subsonic and supersonic flow which can be unstable for certain operating pressure ratios. The unstable flow gives rise to oscillations of pressure and density which occur throughout the length of the duct, including the base or corner regions. These oscillations have been called base pressure oscillations and can occur in both symmetrical and asymmetrical flow. During the oscillations the strength and location of a normal shock in the duct change.

Praca dotyczy badań nieustalonego ściśliwego przepływu w prostokątnym kanale z nagłym rozszerzeniem przekroju poprzecznego. Krytyczny wypływ z krótkiej dwuwymiarowej dyszy zbieżnej do prostokątnego kanału wytwarza w nim mieszany, poddźwiękowy i naddźwiękowy przepływ, który może być niestabilny dla pewnych stosunków ciśnienia. Niestabilność przepływu prowadzi do oscylacji ciśnienia i gęstości wzdłuż całego kanału, łącznie z obszarami zastoju przy dyszy. Oscylacje te nazwano oscylacjami ciśnienia obszaru zastoju i mogą one występować zarówno w przepływie symetrycznym jak i niesymetrycznym. Natężenie i położenie prostopadłej fali uderzeniowej w kanale zmieniają się podczas oscylacji.

Работа касается исследований неустановившегося сжимаемого течения в прямоугольном канале с внезапным расширением поперечного сечения. Звуковое истечение из короткого, двумерного, сходящегося сопла переходит в прямоугольный канал, вызывая смешанное, дозвуковое и сверхзвуковое течение, которое может быть нестабильное для некоторых отношений давления. Нестабильное течение вызывает возникновение осцилляций давления и плотности, которые происходят вдоль канала и в областях мёртвой зоны. Эти осцилляции названы осцилляциями донного давления и могут выступать так в симметричном, как и в несимметричном течении. Во время осцилляций интенсивность и положение нормальной ударной волны в канале изменяются.

1. Introduction

ABRUPT changes in cross-section occur in some kinds of supersonic diffusers, ejector systems, pressure-reducing valves, and exhaust valves of internal combustion engines. Large amplitude oscillations sometimes occur downstream of the abrupt change in section in both circular and rectangular ducts. Several different types of oscillation can occur, but this paper is concerned with a kind which is characterized by a variation in the location and strength of a normal shock in the area of flow reattachment following the sudden expansion. This oscillation takes place throughout the duct, including the base region immediately downstream of the abrupt change in cross-section, and for this reason the oscillation has been referred to as a base pressure oscillation.

The base pressure oscillations occur for a small range of pressure conditions for both short and long ducts. In the case of short ducts a hysteresis exists in the static pressure

conditions. In rectangular ducts oscillations can occur in symmetrical flow, and can also occur when the flow is asymmetrical with a preferred direction to one duct wall.

For the oscillations the non-dimensional ratio $p/\frac{1}{2}\varrho u^2$ is of the order of unity (where p is the amplitude of the oscillation in pressure, ϱ is the density and u the velocity of the flow at a particular point in the duct). For turbulence the above ratio is of the order of 0.01. Hence these are large amplitude oscillations which in certain cases can be a source of intense externally-generated noise [1, 2].

2. Apparatus

The flow was studied in a rectangular duct of a width of 100 mm which is shown schematically in Fig. 1. Atmospheric air at room temperature passed through a short intake (*1*) to a convergent nozzle (*2*). The nozzle was about 20 mm in length, semi-circular in section,

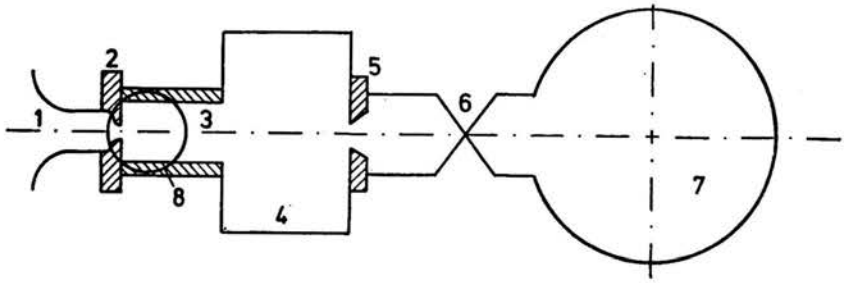

FIG. 1. Schematic diagram of experimental arrangement: *1* — intake, *2* — nozzle, *3* — test duct, *4* — plenum chamber, *5* — throttle, *6* — gate valve, *7* — vacuum chamber, *8* — optical window.

and designed to produce a thin boundary layer at the exit. The test duct (*3*) had a larger cross-section so that the flow suffered an abrupt expansion as it left the nozzle. The test section was followed by a plenum chamber (*4*) in which the pressure could be maintained constant by a control valve (*5*). The plenum chamber could be quickly connected to a vacuum chamber of volume 132 m³ (*7*) by a pneumatically-operated gate valve (*6*).

A Mach-Zehnder interferometer was used to study the flow field in the duct. Photographs could be taken using a spark light source in a chamber of argon, which had a duration of 1 μs.

Pressure fluctuations were measured by quartz piezo-electric transducers placed on the upper or lower surface of the duct. These signals were recorded on an FM magnetic

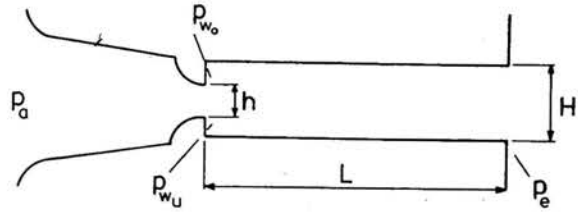

FIG. 2. Static pressure notation and geometrical parameters.

tape recorder. The frequency spectra were then obtained using a Hewlett Packard Fourier Analyser. The Analyser has a dual input capability and can be used to obtain cross-spectra, and hence the phase difference between two signals.

The main geometrical parameters of the duct are shown in Fig. 2, together with some important static pressures which could be measured with mercury manometers.

3. Static pressure conditions

Figures 3 and 4 show static pressures in the base region of the duct as a function of p_e/p_a (i.e. the reciprocal of the pressure ratio across the nozzle and duct) for duct lengths of 160 mm and 240 mm respectively. The area ratio ϕ in both cases was 0.3, where $\phi = h/H$.

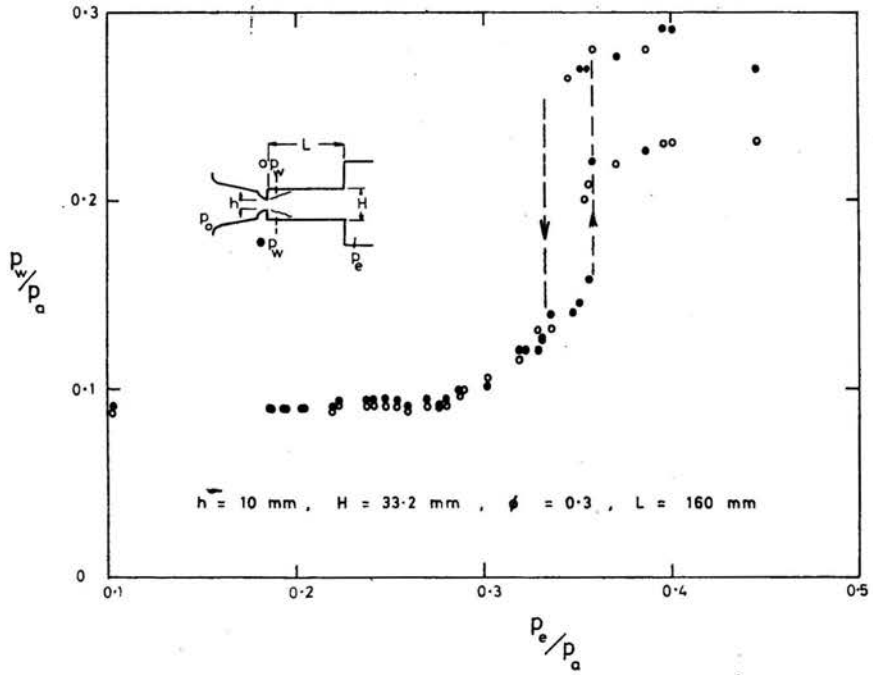

FIG. 3. Variation of base pressure with receiver pressure, $h = 10$ mm, $H = 33.2$ mm, $\phi = 0.3$, $L = 160$ mm.

A main characteristic of such rectangular ducts is the hysteresis in the base pressure. At high values of p_e/p_a the flow is asymmetrical, but attachment occurs as the pressure ratio is decreased. With increasing values of p_e/p_a separation occurs at a pressure ratio slightly higher than that at which attachment occurred. With the longer duct of Fig. 4 the base pressure of the symmetrical flow immediately after attachment is approximately the mean of the base pressures of the asymmetric flow just prior to attachment.

The pressure ratios at which the discontinuities occur depend to some extent on the construction of the nozzle and duct. Slight variations occur after the nozzle has been dismantled and reconstructed.

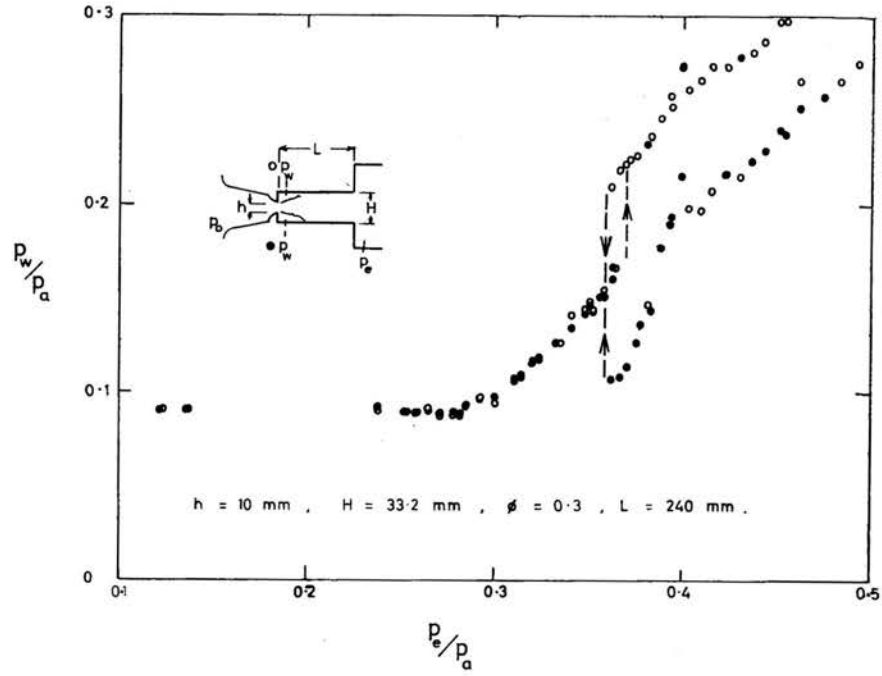

FIG. 4. Variation of base pressure with receiver pressure, $h = 10$ mm, $H = 33.2$ mm, $\phi = 0.3$, $L = 240$ mm.

4. Flow patterns

Some of the flow patterns in the duct are shown in the interferograms of Fig. 5. At high values of p_e/p_a the flow is asymmetric (Fig. 5a, where p_e/p_a is 0.40). With decreasing p_e/p_a the flow becomes attached and is characterized by a single normal shock wave in the duct near the nozzle exit. In Fig. 5b the flow is unstable and the shock wave position and strength vary. This type of oscillation is called symmetrical base pressure oscillation, and a sequence of interferograms for a cycle may be studied in a previous paper [3]. The base pressure oscillation occurs over a small range of pressure ratios, mainly in the area of the lower branch of the hysteresis loop. Thus for a duct of a length of 160 mm oscillations occur for a pressure ratio p_e/p_a range from 0.334 to 0.358. For a duct of a length of 240 mm the corresponding range is 0.351 to 0.367. The variation in pressure occurs throughout the duct, including the base region.

In Fig. 5c the pressure ratio p_e/p_a has been reduced and a stable flow has resulted. Figure 5c differs from 5b, which is an instantaneous photograph taken during a cycle, in that shock waves stretch almost entirely across the duct, and the flow at the boundaries downstream of the shock waves is supersonic. Thus it is no longer possible for a disturbance to travel upstream into the base region.

At low values of the pressure ratio p_e/p_a the base pressure is constant and the flow pattern is characterized by series of reflected oblique shocks, (see Fig. 5d). In between the

conditions represented by Figs. 5c and 5d there are other flow patterns and oscillations, but these will not be described here. For the longer duct of a length of 240 mm oscillations of the base pressure kind occur in asymmetrical flow at pressure ratios from 0.371 to 0.377.

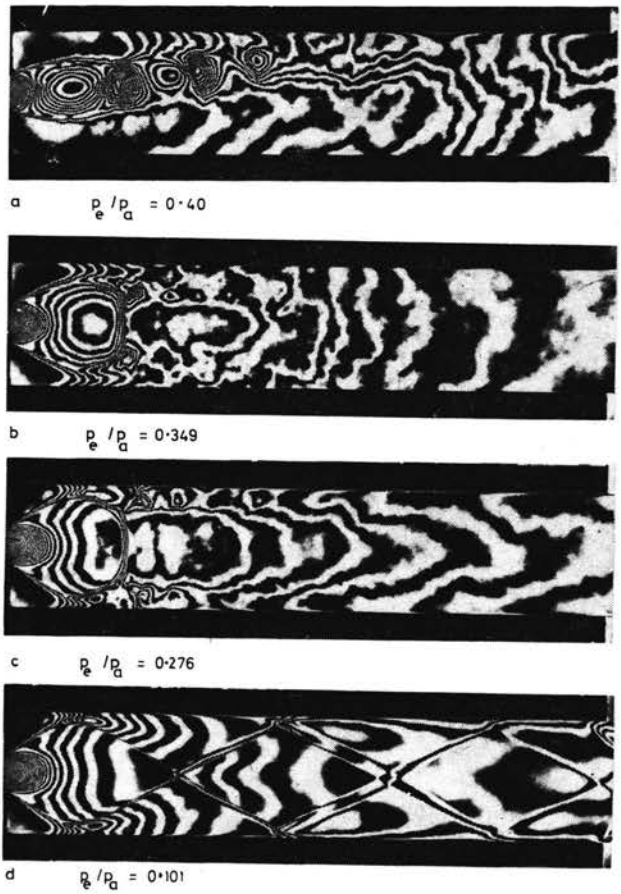

FIG. 5. Flow patterns, $h = 10$ mm, $H = 33.2$ mm, $\phi = 0.3$, $L = 160$ mm, a) $p_e/p_a = 0.40$, b) $p_e/p_a = 0.349$, c) $p_e/p_a = 0.276$, d) $p_e/p_a = 0.101$.

5. Symmetrical base pressure oscillations

The variations in the pressure fluctuations on the upper and lower surfaces of the duct can be studied with reference to Fig. 6. Here the pressure ratio p_e/p_a was 0.364 and the duct length 240 mm and area ratio $\phi = 0.3$. Two Mach-Zehnder interferograms taken at different stages in the cycle are also shown. On the lower surface of the duct piezo-electric pressure transducers were placed at 8, 38, 68, 98 and 123 mm from the base, and are referred to as positions A, B, C, D and E, respectively. Transducers H, I and J at 8, 38 and 98 mm from the base were positioned on the upper surface. The presence of higher frequency components can be seen, particularly at the downstream transducer locations.

In the lower interferogram shown in Fig. 6 the normal shock wave is close to the base, and the pressure at A is low. Surrounding the subsonic central flow are supersonic regions at the extremities of the normal shock and, during the cycle, these move towards the walls when the pressure at A has the lowest value. In the upper interferogram the shock wave has moved to the right, is weaker, and allows the pressures at A and H to be higher.

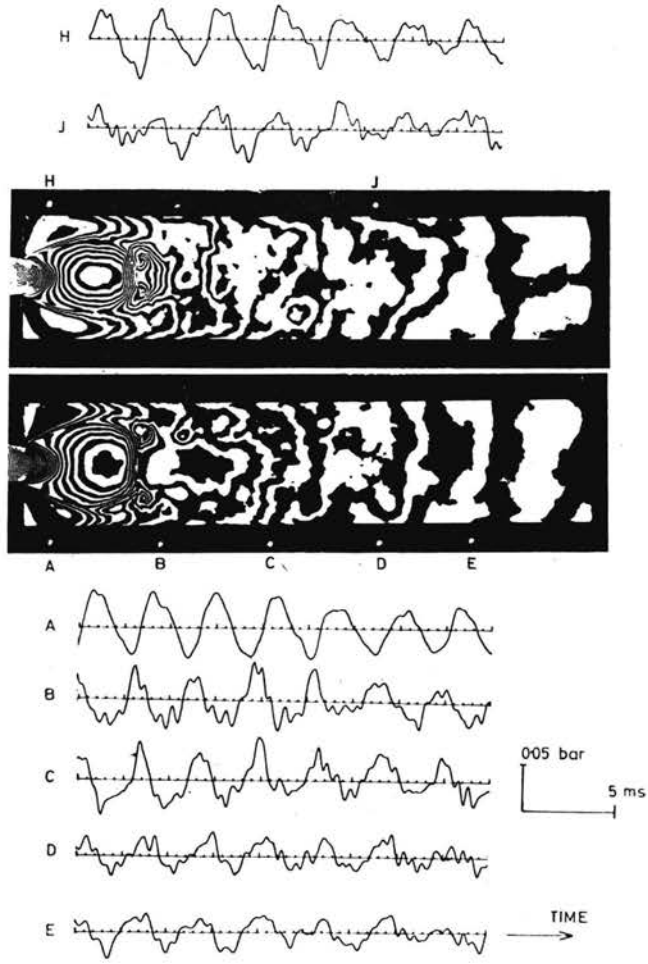

FIG. 6. Interferograms and surface pressure fluctuations for symmetrical base pressure oscillations $h = 10$ mm, $H = 33.2$ mm, $\phi = 0.3$, $L = 240$ mm, $p_e/p_a = 0.364$.

Power spectra obtained from pressure-time signals similar to those of Fig. 6 are shown in Fig. 7. These spectra were obtained by taking an average of 64 separate spectra over a period of 16 s. The effective resolution was 4 Hz. Exact harmonics are present at 320, 640, 960 Hz, etc. The higher harmonics are more noticeable at the downstream transducer locations. For a given operating pressure ratio the frequency of the oscillation is fairly steady, and does not vary much with time.

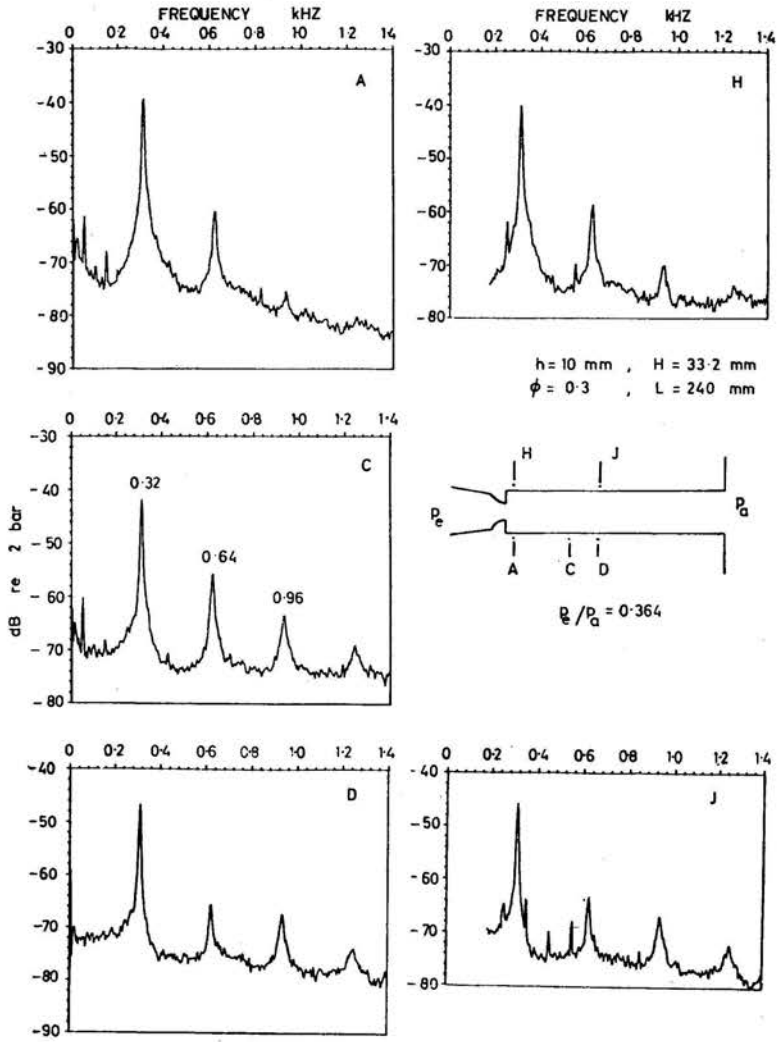

FIG. 7. Power spectra of surface pressure fluctuations for symmetrical base pressure oscillations, $h = 10$ mm, $H = 33.2$ mm, $\phi = 0.3$, $L = 240$ mm, $p_e/p_a = 0.364$.

Approximate information on the relative phases of the pressure signals can be obtained from visual observation of the traces in Fig. 6, but more exact phase changes can be determined from the cross-power spectra. The advantage of the cross-power method is that phase information for each harmonic can be determined. With the pressure signal at transducer position B as a reference the following phase information, presented in Table 1, was obtained for the fundamental and second harmonic for the duct of a length of 240 mm and a pressure ratio p_e/p_a of 0.364.

For the fundamental it can be seen that B and A are considerably out of phase, and that the downstream transducers C, D and E have phase differences with respect to B of the same order. This indicates that B represents a dividing point. B is of course, close to the position of the normal shock which is the centre of the oscillation.

Table 1.

	Fundamental		Second harmonic
Y	angle in degrees by which *Y* lags *B*	*Y*	angle in degrees by which *Y* lags *B*
A	138	*A*	180
C	42	*C*	130
D	80	*D*	210
E	64	*E*	225
Y	angle in degrees by which *Y* lags *I*	*Y*	angle in degrees by which *Y* lags *I*
H	127	*H*	170
J	93	*J*	260

6. Asymmetrical base pressure oscillations

Similar oscillations can be obtained in asymmetrical flow. For example, for a duct of a length of 240 mm asymmetrical base pressure oscillations exist for the pressure ratio p_e/p_a from 0.371 to 0.377. During a cycle the flow structure changes from a cellular type, similar to that of a free, supersonic jet, to a flow with supersonic regions at the extremities of the first normal shock. In the former structure two cells are usually formed, and the latter structure is similar to the lower interferogram of Fig. 6, although the normal shock is stronger in the asymmetrical case, as the oscillation is concentrated on one side.

The power spectra of the pressure transducer signals for the asymmetrical base pressure oscillations are shown in Fig. 8. The most prominent frequencies are the fundamental and third harmonic, although the third harmonic is only strong in the region close to the base.

Table 2.

	Fundamental	Third harmonic
Y	amount by which *Y* lags *B* (degrees)	amount by which *Y* lags *B* (degrees)
A	155	172
C	48	225
D	35	280
E	25	—
	amount by which *Y* lags *I* (degrees)	amount by which *Y* lags *I* (degrees)
H	28	68
J	320	170

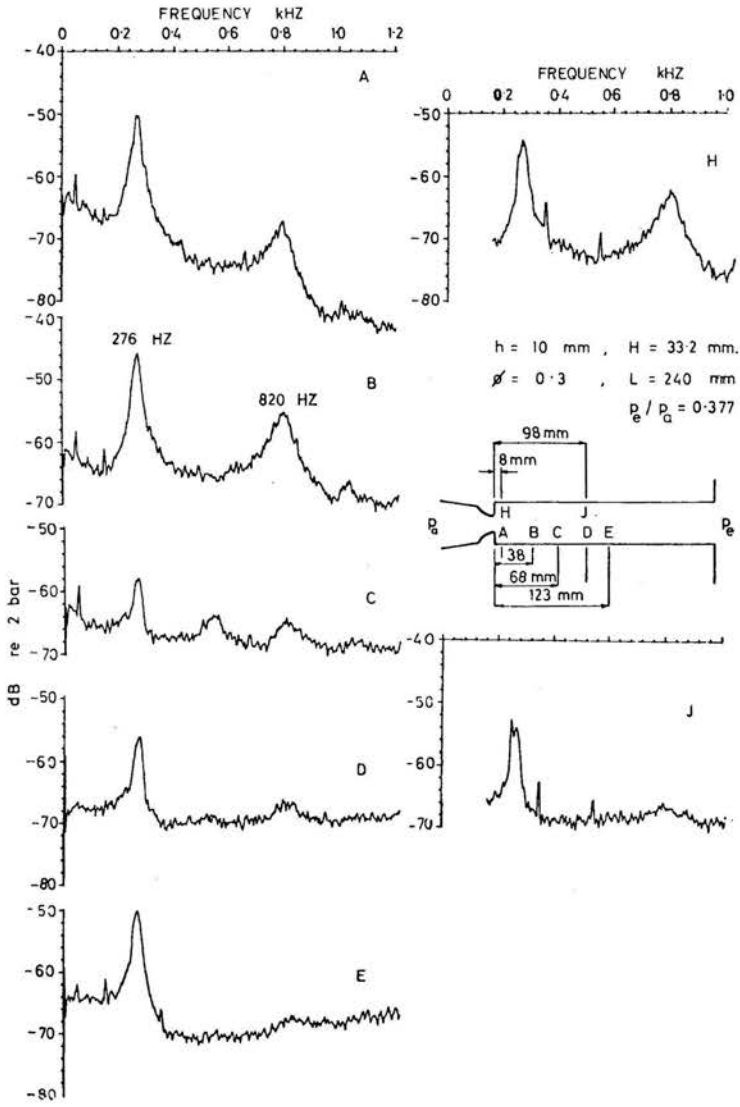

FIG. 8. Power spectra of surface pressure fluctuations for asymmetrical base pressure oscillations, $h = 10$ mm, $H = 33.2$ mm, $\phi = 0.3$, $L = 240$ mm, $p_e/p_a = 0.377$.

The fundamental frequency is lower in the case of the asymmetrical flow than for the symmetrical case, 276 Hz compared with 320 Hz. A possible explanation is that the Mach number M on the attached side during asymmetrical oscillations is greater than the equivalent Mach number in symmetrical flow. With a mean flow in a duct the natural frequencies are modified by a factor of $1-M^2$, and so for a higher Mach number a lower frequency results.

The shorter duct of a length of 160 mm did not exhibit asymmetrical oscillation. Observation indicates that a base pressure variation of the kind shown in Fig. 4 is required, if

asymmetrical oscillations are to occur. Only with the static variation type as in Fig. 4 is it possible to have a local Mach number on the attached side greater than for symmetrical flows at similar pressure ratios.

As in the case of symmetrical base pressure oscillations cross-power spectra have been used to determine phase information, which is presented in Table 2.

With asymmetrical oscillations phase information is difficult to interpret, because there is not a uniform flow in the duct. As with the symmetrical oscillations there is the same large phase difference between B and A on the attached side, but on the unattached side the phase difference between the two equivalent points, I and H, is much smaller.

7. Variation of surface static pressure along the duct

Figure 9 shows how the time-averaged surface static pressure varies along the duct for the case of base pressure oscillation and for a stable flow. An interferogram at an instant during the oscillatory flow is shown with the same length scale. The pressure rise

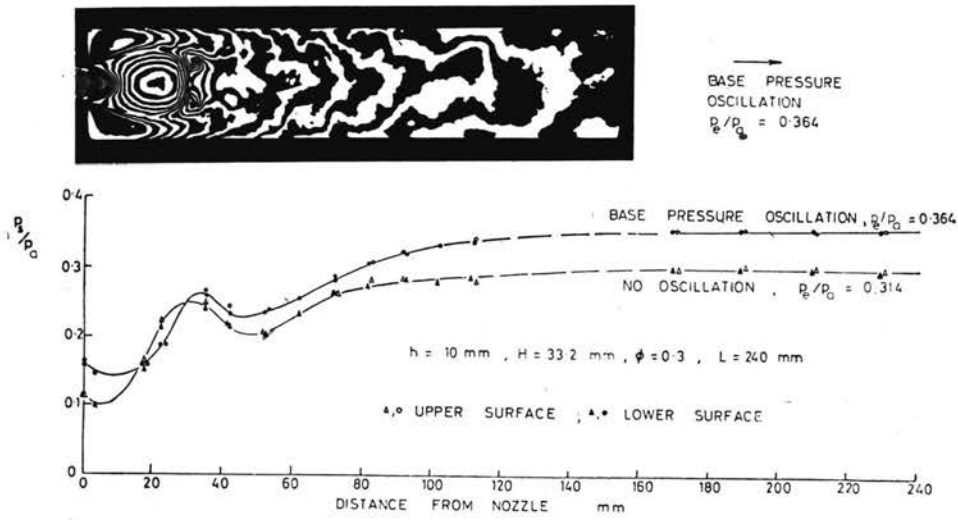

FIG. 9. Time-averaged surface static pressures along the duct for symmetrical base pressure oscillations, $h = 10$ mm, $H = 33.2$ mm, $\phi = 0.3$, $L = 240$ mm, $p_e/p_a = 0.364$.

across the shock is followed by a decrease in static pressure as the flow separates. In the case of asymmetrical oscillations, shown in Fig. 10, there is a similar static pressure rise on the attached side. There is some evidence of two peaks which correspond to the two normal shocks of the cellular structure.

The pressure p_H after the shock shows some evidence of increasing with the base pressure p_W to a maximum value (see Fig. 11, in which p^* is the nozzle critical pressure). The data for Fig. 11 were obtained from static pressure profiles along the duct walls, of the kind shown in Fig. 9, and refer to symmetrical base pressure oscillations. What is really

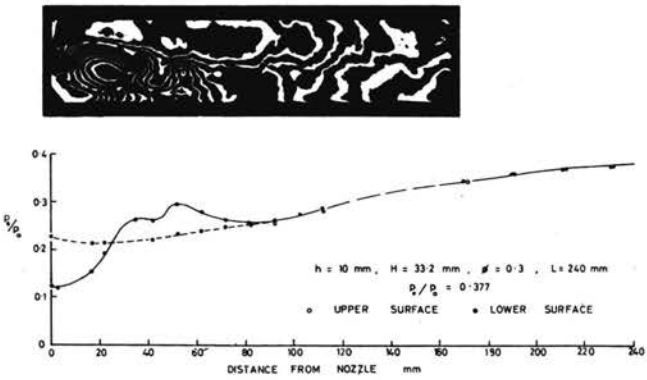

FIG. 10. Time-averaged surface static pressure along the duct for asymmetrical base pressure oscillations, $h = 10$ mm, $H = 33.2$ mm, $\phi = 0.3$, $L = 240$ mm, $p_e/p_a = 0.377$.

required is the static pressure rise along the centre line of the duct. The density distribution along the centre line [3] indicates that the actual increase in pressure is much more sudden than that shown in Fig. 9, thus Fig. 11 must be regarded as only approximate.

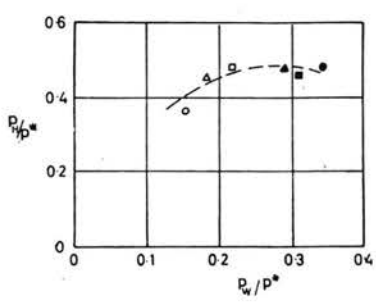

	ϕ	l mm	p_e/p_a
○	0.3	240	0.31
●	0.3	240	0.373
△	0.3	240	0.314
▲	0.2	240	0.364
□	0.3	200	0.334
■	0.3	200	0.366

(Closed symbols indicate oscillation).

FIG. 11. Variation of the static pressure after the normal shock p_H with the base pressure p_W for symmetrical base pressure oscillations.

8. Theoretical model

The aim of the present model of the flow is to obtain from numerical calculations oscillations with variables similar in magnitude to those obtained in the experiments. The idealized geometry of the flow is shown in Fig. 12. The jet boundaries and the shock wave are approximated by straight lines. The basic equations in the calculation comprise the equations of continuity, momenta in the transverse and axial directions, and also of momentum along the jet boundary. Additionally the relation between the shock position X_s and the shock velocity U_s is introduced in the form $dX_s/dt = U_s$. The equations of continuity and momentum are used in the integral form and applied to the flow field within the dashed line in Fig. 12. In order to solve the integrals in the basic equations, the integrands are approximated by linear functions in two directions, first from the axis to the boundary of the jet and then from the enlargement to the shock position. The re-

sulting approximate equations are ordinary differential equations in time t with the variables X_s, U_s, base pressure p_W, velocity and density on the axis upstream of the shock wave, and the velocity on the jet boundary upstream of the shock wave. Five equations are ob-

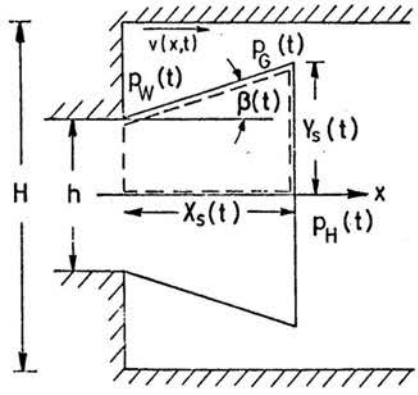

FIG. 12. Flow field of the theoretical model.

tained for these six variables and, additionally, a relation between the base pressure p_W and the pressure p_H downstream of the shock is postulated. For this feedback between p_H and p_W different model equations have been developed and tested by numerical calculations [4]. One of these model equations will be discussed here.

The extra model equation for the feedback can be obtained by considering the incompressible flow in the dead air caused by the expansion and contraction of the supersonic part of the flow field. The driving pressure difference in the flow direction is assumed to be $p_W - p_G$. In the calculation of the flow the Bernoulli equation for unsteady flow is used and

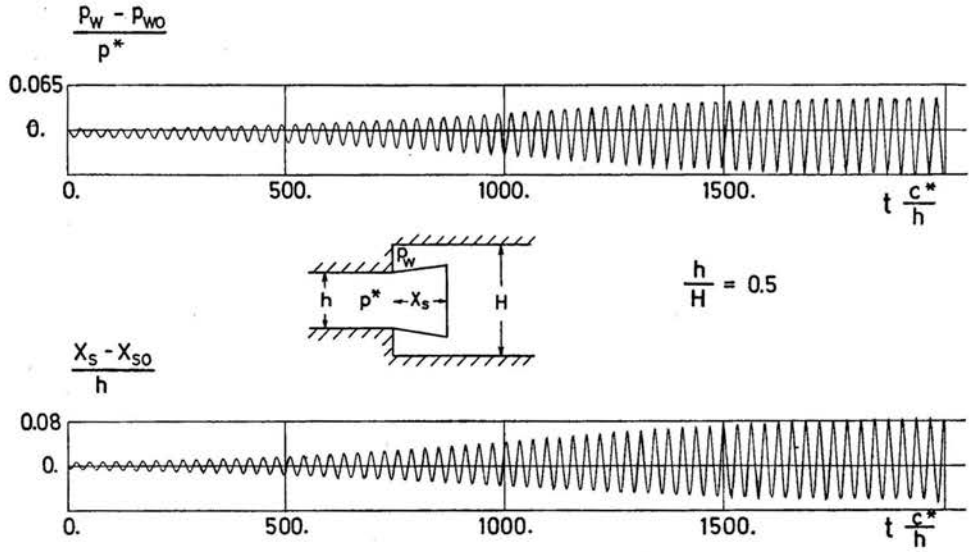

FIG. 13. Base pressure and shock distance variations starting from slightly disturbed steady flow and finally approaching a limiting amplitude, $h/H = \phi = 0.5$.

the velocity $v(x, t)$ is determined by a one-dimensional continuity equation. In addition, it is assumed that the relationship between the pressure p_H downstream of the shock and the pressure p_G is the same for unsteady flow as for steady flow. To a first approximation the equation $p_G = Kp_H$, where K is a constant defined by the initial steady flow, is assumed. The equations for the steady initial flow field are derived from the differential equations by cancelling the derivatives of time. A value of p_W is chosen, and hence associated values of the other variables are established which satisfy the steady conditions. A disturbance is introduced into the unsteady system of equations by artificially changing one of the variables from its equilibrium value. As a result of this disturbance there is either an attenuation of the variable parameters or an amplification which leads to the onset of a constant amplitude oscillation.

The following results have been obtained from the numerical calculations:

(i) a distortion of the steady flow with $p_W/p^* < k \approx 0.55$ is attenuated (p^* is the critical pressure),

(ii) for $p_W/p^* > k \approx 0.55$ the oscillation builds up to a final limit cycle oscillation of constant amplitude (see Fig. 13),

(iii) the frequency of the oscillations is of the same order as those observed in the experiments (see Fig. 14).

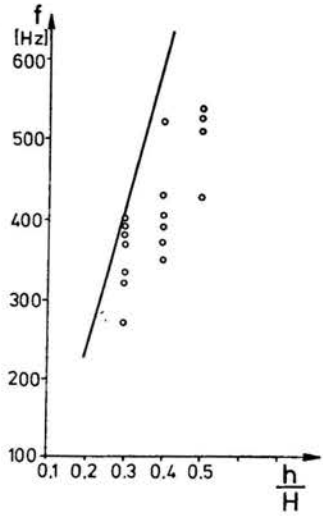

FIG. 14. Frequency of the self-excited oscillation. ∘ Experimental results for different duct lengths and $h = 10$ mm, — results according to the theoretical model with $h = 10$ mm.

9. Discussion of the oscillation mechanism

The experimental and theoretical investigations lead to the following idea about the oscillation mechanism and the feedback loop: if the pressure is decreasing in the dead air region, the supersonic jet will expand, and the pressure upstream of the shock wave may decrease. Up to a certain value a lower pressure p_A in front of the shock wave causes a higher pressure p_H downstream of the shock (negative response). A larger pressure p_H behind the shock tends to increase the pressure p_W in the dead air, as the two regions

are connected through the boundary layer. The base prossure p_W is closely related to the pressure p_A in front of the shock wave, and hence a feedback loop is formed with a certain internal time delay. This feedback system works only in the case of a negative response. This idea of a negative response is incorporated in Fig. 15 which is obtained from

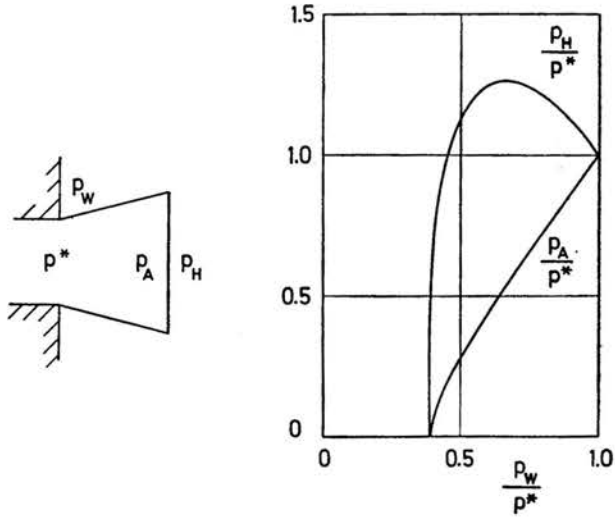

FIG. 15. Solution of the steady flow equations.

the solution of the steady flow equations. The limit cycle oscillations occur for values of $p_W/p^* > 0.55$, which is in the area of the negative response. The only experimental evidence of a negative slope is presented in Fig. 11. This evidence, which is based on limited experimental data, cannot be regarded as convincing, but it does point to a possible confirmation of the theoretical curve of p_H against p_W. Exact agreement between experiment and a theoretical model of this kind is not expected, because of the approximations introduced into the model.

The experiments have shown a strong dependence of the frequency upon the duct length. In the present theoretical model the duct length is not included, but only the geometry of the abrupt expansion. In the model the supersonic flow terminating in the shock wave acts as the generator of the oscillations. The duct provides a system which can act as a resonator, either amplifying or attenuating the input. The final oscillation depends upon both the supersonic oscillator and the duct.

From the calculated frequency it is possible to use the equation for the resonant frequencies of a duct with flow, and hence obtain the length of a "resonant duct". Hence it can be seen if the resonant frequency and its harmonics for a given duct are synchronizing with the supersonic generator.

10. Concluding remarks

The existence of large amplitude oscillations has been established in supersonic flow in a rectangular duct which is immediately downstream of a nozzle of smaller cross-section,

in which sonic flow exists at the exit. These oscillations exist throughout the entire length of the duct, and have been called base pressure oscillations.

The base pressure oscillations are self-excited and a theoretical model has been devised to give an explanation of the mechanism. The generator of the oscillation has been modelled by considering the expansion region of the jet from the nozzle. The supersonic flow terminates in a normal shock wave and can be shown to be unstable, and hence a source of oscillation in certain pressure ranges. The duct then amplifies or attenuates the original oscillation.

References

1. J. S. ANDERSON, T. J. WILLIAMS, *Base pressure and noise produced by the abrupt expansion of air in a cylindrical duct*, J. Mech. Engng. Sci., **10**, 262–268, 1968.
2. K. J. WITCZAK, *Krytyczny wypływ gazu do przewodu jako źródło hałasu*, Dr. Thesis, Technical University of Warsaw, 1975.
3. J. S. ANDERSON, W. M. JUNGOWSKI, W. J. HILLER and G. E. A. MEIER, *Flow oscillations in a duct with a rectangular cross-section*, J. Fluid Mech., **79**, 769–784, 1977.
4. G. GRABITZ, *Über die Entstehung selbsterregter Schwingungen einer Überschallströmung in einem Kanal mit plötzlicher Querschnittserweiterung*, Max-Planck-Institut für Strömungsforschung, Göttingen, Bericht 14/1976, 1976.

THE CITY UNIVERSITY, LONDON, GREAT BRITAIN,
MAX-PLANCK-INSTITUT FÜR STRÖMUNGSFORSCHUNG, GÖTTINGEN, FRG,
and
WARSAW TECHNICAL UNIVERSITY, WARSZAWA, POLAND.

Received September 27, 1977.